CrystEngComm

Cite this: *CrystEngComm*, 2012, **14**, 4989–4996

www.rsc.org/crystengcomm

PAPER

Anions make the difference: conversion from zero- to one-dimensional structures and luminescent properties of lanthanide-based complexes†

Xuhuan Yan, Zhenzhong Yan, Ye Zhang, Weisheng Liu, Yu Tang* and Minyu Tan

Received 14th February 2012, Accepted 25th April 2012
DOI: 10.1039/c2ce25210d

Reaction of a newly designed amide type ligand, benzyl-*N*,*N*-bis[(2′-benzylaminofomyl)-phenoxyl)ethyl]-amine (**L**) with lanthanide nitrates and picrates has produced two isostructural series of lanthanide coordination compounds, $[Ln_2\mathbf{L}_2(NO_3)_6(DMF)_2]_n$ [series 1, monoclinic $P2_1/c$, Ln = Pr (**1**), Sm (**2**), Eu (**3**), Tb (**4**), and Dy (**5**)] and $[Ln\mathbf{L}(pic)_3(CH_3CH_2OH)]_n$ [series 2, triclinic $P\bar{1}$, Ln = Nd (**6**), Eu (**7**), Tb (**8**), and Er (**9**)]. Series 1 have zero-dimensional (0D) dinuclear rectangular macrocycle architectures, while series 2 exhibit one-dimensional (1D) chain patterns. Meanwhile, the two series of structures are further connected through weak intermolecular hydrogen bonds to yield three-dimensional (3D) supramolecular structures. The variations from zero- to one-dimensional coordination structures are attributed to different steric confinement of the nitrate and picrate anions. In addition, we have studied the luminescent properties of the nitrate and picrate complexes, and found that the picrate complexes give very weak luminescence due to coordinated ethanol molecules existing in complexes, which decrease the luminescence. So, herein the luminescent properties of only the Sm (**2**), Eu (**3**), Tb (**4**), and Dy (**5**) nitrate complexes are investigated in detail.

Introduction

The preparation of coordination polymers has been provoking considerable current interest during the past decades, owing to their enormous variety of intriguing structural topologies as well as great potential applications in the area of catalysis, gas storage, separation.[1] From the viewpoint of crystal engineering, the key to coordination polymers with desired topologies and physicochemical properties is to choose appropriate metal ions and organic building blocks for an effective assembly. As functional metal centers, lanthanide ions are helpful in the formation of unusual molecular architectures due to their high coordination numbers and variable coordination geometry (which also make it difficult to control the preparation of lanthanide coordination polymers, though). The other advantages of lanthanides are their long excited-state lifetimes, high chromaticities (especially, Sm(III), Eu(III), Tb(III), and Dy(III)) and brightest emission with some organic ligands, which are also pertinent to applications in the domain of solid-state photonic materials.[2] On the other hand, amide type ligands have been extensively applied in preparing lanthanide complexes. The complexes possess novel coordination structures and exceptional luminescent properties, because of their versatile coordination modes, predictable patterns of hydrogen bonding donors and acceptors and good light absorptivity.[3]

Anions also play an important role in preparing lanthanide coordination polymers with fantastic coordination polymeric architectures,[3a,4] in addition to metal ions and organic ligands. The anions can be divided into having two key effects upon the structures of the final coordination polymers. Firstly, the anions, that can coordinate to metal cations, obviously influence the coordination sphere of the metal cations and hence the construction of networks. Secondly, the size of the anions can influence the long-range order and degree of interpenetration of the lanthanide coordination polymers. Previously, we reported two anion-induced chiral lanthanide-organic frameworks assembled by an achiral amide type tripodal ligand.[3a] Inspired by the aforementioned progress, we were prompted to design and prepare a new conformationally flexible amide type ligand benzyl-*N*,*N*-bis[(2′-benzylaminofomyl)phenoxyl)ethyl]-amine (**L**) (Scheme 1). The amide type ligands with several (generally 2–4) identical arms have been intensively studied,[3a–i] but ligands with three incompletely identical arms such as ligand **L** here are

Key Laboratory of Nonferrous Metal Chemistry and Resources Utilization of Gansu Province, State Key Laboratory of Applied Organic Chemistry and College of Chemistry and Chemical Engineering Lanzhou University, Lanzhou, 730000, P. R. China. E-mail: tangyu@lzu.edu.cn; Fax: +86-931-8912582; Tel: +86-931-8912552

† Electronic supplementary information (ESI) available: theoretical details of "shape-measure" *S*, the intrinsic quantum yield of the Eu(III) complex, tables of selected bond distances and angles, hydrogen bonds in crystal packing of the complexes, the powder X-ray diffraction patterns of the Gd and Tb (**4**) nitrate complexes, the intramolecular π–π stacking interactions in compound **4**, 2D supramolecular layer and 3D framework generated by intermolecular hydrogen bonds, luminescence decay curves of the complexes, excitation and emission spectra of the Tb(III) nitrate complex in different solutions at room temperature, absorption spectra of the ligand, phosphorescence spectrum of the compound $[Gd\mathbf{L}(NO_3)_6]\cdot H_2O$. CCDC reference numbers 666992–666995, 788729, and 852907–852910. For ESI and crystallographic data in CIF or other electronic format see DOI: 10.1039/c2ce25210d

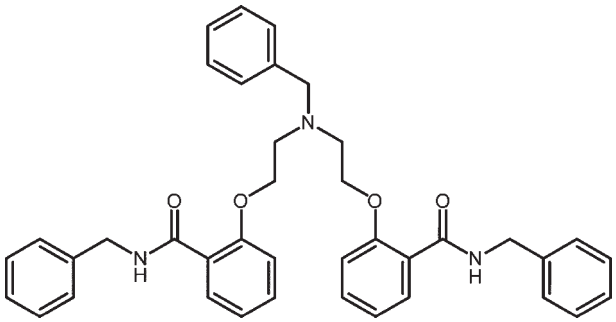

Scheme 1 A schematic illustration of the ligand **L**.

rather rare.[4c] Moreover, the ligand **L** with two well flexible amide type arms can construct discrete structures or coordination polymers. We selected two different anions (small inorganic nitrate and large organic picrate) for further comparison because they have similar coordination modes (monodentate or bidentate coordination mode, and the coordination sites are the oxygen atoms). We expected to investigate how the anions influenced supramolecular self-assembly of lanthanide complexes as well as their luminescent properties. In this report, we constructed two series of new coordination compounds with lanthanide nitrate and picrate. The single crystal X-ray diffractions shows that the crystal structures of $[Ln_2\mathbf{L}_2(NO_3)_6(DMF)_2]_n$ [Ln = Pr (**1**), Sm (**2**), Eu (**3**), Tb (**4**), and Dy (**5**)] form interesting zero-dimensional (0D) dinuclear [2+2] rectangular macrocyclic structures. However, the structures of $[Ln\mathbf{L}(pic)_3(CH_3CH_2OH)]_n$ [Ln = Nd (**6**), Eu (**7**), Tb (**8**), and Er (**9**)] confirm one-dimensional (1D) linear coordination polymers. Moreover, the solid state luminescent properties of the complexes **2**, **3**, **4**, and **5** at the room temperature were also investigated in detail and correlated with the triplet energy level of the designed ligand.

Experimental section

Materials and instrumentation

N-benzylsalicylamide,[5] β,β'-dichlorodiethylamine hydrochloride salt,[6] lanthanide nitrates[7] and lanthanide picrates[8] (***CAUTION!*** *Although we have experienced no problems in handling picrate compounds, these should be handled with great caution due to the potential for explosion*) were prepared according to the literature methods, respectively. Other chemicals were obtained from commercial sources and used without further purification. ^{1}H NMR spectrum was measured on a Varian Mercury-300B spectrometer in d-chlorform solution with tetramethylsilane $[Si(CH_3)_4]$ as an internal standard. Elemental analyses were determined on an Elementar Vario EL analyzer. The FT-IR spectra were recorded on a Nicolet 360 FT-IR spectrometer using KBr pellets in the range of 4000–400 cm^{-1}. Powder X-ray diffraction patterns (PXRD) were determined with Rigaku-Dmax 2400 diffractometer using Cu-Kα radiation. Mass spectra were recorded on Bruker UHR-TOF maXis 4G Mass spectrometer. The solid state luminescence spectra of Sm (**2**), Eu (**3**), Tb (**4**), and Dy (**5**) complexes (the excitation and emission slit widths were 1.0 and 1.0 nm except for the Sm (**2**) complex, with the excitation and emission slit widths being 2.5 and 1.0 nm), solution luminescence spectra of the Tb nitrate complex (concentration: 1.0×10^{-3} mol L^{-1}, the excitation and emission slit widths were 5.0 and 2.5 nm) and phosphorescence spectrum of the Gd nitrate complex were obtained on a Hitachi F-4500 fluorescence spectrophotometer. UV/vis absorption spectra were determined on a Varian UV-Cary100 spectrophotometer. The quantum yields of the complexes were determined by an absolute method using an integrating sphere (150 mm diameter, $BaSO_4$ coating) from Edinburgh Instruments FLS920. The lifetime measurement was measured on an Edinburgh Instruments FLS920 Fluorescence Spectrometer with a Nd pumped OPOlette laser as the excitation source.

Preparation of the ligand L

The β,β'-dichlorodiethylamine hydrochloride salt (1 mmol) and potassium carbonate (2 mmol) were refluxed in acetone (25 cm^3) for 30 min, and then the benzyl bromide (1 mmol) was added to the solution. The reaction mixture was refluxed for 12 h and the hot solution was filtered off. The collected organic phase was evaporated in a vacuum. Then the obtained product was added to a mixture of *N*-benzylsalicylamide (2.0 mmol), potassium carbonate (4 mmol) and dry dimethylformamide (DMF) (20 cm^3) which was warmed to 90 °C, and the reaction mixture was stirred at 90 °C for 12 h. After cooling down, the mixture was poured into water (100 cm^3). The resulted solid was treated with column chromatography on silica gel [petroleum ether : ethyl acetate (3 : 2)] to get the ligand **L**, yield 80%, m. p. 124–125 °C; Anal. Calcd for $C_{39}H_{39}O_4N_3$: C, 76.32; H, 6.40; N, 6.85. Found: C, 76.39; H, 6.18; N, 6.51. ^{1}H NMR ($CDCl_3$, 300MHz): 2.65–2.69 (t, 4H), 3.47–3.49 (s, 2H), 3.88–3.92 (t, 4H), 4.60–4.62 (d, 4H), 6.63–7.38 (m, 23H), 8.21–8.27 (q, 2H); IR (KBr pellet, cm^{-1}): 3330 m, 1636 s, 1600 m, 1531 m, 1488 m, 1449 m, 1307 m, 1237 m, 1106 w, 822 w, 753 s, 697 m.

Synthesis of the lanthanide complexes

$[LnL(NO_3)_3]\cdot H_2O$. An ethyl acetate solution (5 cm^3) of $Ln(NO_3)_3\cdot 6H_2O$ (Ln = Pr, Sm, Eu, Gd, Tb, and Dy) (0.1 mmol) was added dropwise to a solution of 0.1 mmol ligand **L** in ethyl acetate (5 cm^3). The mixture was stirred at room temperature for 8 h, and then the precipitated solid complex was filtered, washed with ethyl acetate, dried *in vacuo* over P_4O_{10} for 48 h and submitted for elemental analyses, yield: 62–75%. The six complexes have similar IR spectra, of which the characteristic bands have similar shifts, suggesting that they have a similar coordination structure. IR (KBr pellet, cm^{-1}) for the Eu nitrate complex as a representative example: 3362 m, 1614 s, 1477 m, 1304 m, 1239 m, 1112 w, 1029 w, 816 w, 754 s, 702 s .

$[LnL(pic)_3]\cdot nH_2O$ (n = 1 or 2). A solution of $Ln(pic)_3\cdot 6H_2O$ (Ln = Nd, Eu, Tb, and Er) (0.1 mol) in ethanol (5 cm^3) was added to a solution of 0.1 mmol ligand **L** in ethanol (5 cm^3). The mixture was stirred at room temperature overnight and the resulting yellow precipitate filtered off, washed with ethanol and dried *in vacuo* over P_4O_{10} for 48 h and submitted for elemental analyses, yield: 60–77%. The four lanthanide picrate complexes have similar IR spectra, suggesting that they are isostructural. IR (KBr pellet, cm^{-1}) for Eu picrate complex as a representative example: 3375 m, 1611 s, 1570 m, 1540 s, 1361 s, 1331 s, 1274 s, 1111 w, 703 s.

Elemental analytical and IR (C=O) spectral data for the newly synthesized lanthanide solid complexes are summarized in Table 1.

Single-crystal X-ray crystallography

Single crystals of the complexes were obtained from a mixed solution of ethanol and DMF solution by slow evaporation for about three weeks at room temperature. The X-ray single-crystal data collections were performed using a Bruker SMART CCD detector diffractometer using graphite-monochromatic Mo-Kα radiation at 294 K. The structures were solved by direct methods and refined by full-matrix least-squares on F^2 using the SHELXS-97 and SHELXL-97 programs.[9] Anisotropic thermal parameters were assigned to all non-hydrogen atoms. The hydrogen atoms were placed in idealized positions and located in the difference Fourier map. Standard DFIX restraints were used for the distance of the disordered atoms, such as (C46 and C47) for compound **2**, (C35 and C10) for compound **3** and (H50 and O5) for compound **7**. Crystallographic data as well as details of data collection and refinement for these complexes are summarized in Tables S1 and S2 (ESI†). Important bond lengths bond angles are listed in Table S3 (ESI†). Hydrogen bonds in crystal packing for the compounds **1–9** are listed in Table S4 (ESI†). CCDC 788729 (**1**), 666992 (**2**), 666993 (**3**), 666994 (**4**), 666995 (**5**), 852907 (**6**), 852908 (**7**), 852909 (**8**), and 852910 (**9**) contain the supplementary crystallographic data for this paper.†

Results and discussion

Synthesis and characterization

Lanthanide nitrate complexes (Ln = Pr, Sm, Eu, Gd, Tb, and Dy) were obtained by the reaction of lanthanide nitrates with **L** in ethyl acetate, and lanthanide picrate complexes (Ln = Nd, Eu, Tb, and Er) were synthesized in ethanol. The obtained complexes are highly stable in air. The solid powders of the lanthanide nitrate complexes are soluble in DMF, DMSO, methanol, ethanol, and acetone, slightly soluble in acetonitrile, but insoluble in $CHCl_3$ and diethyl ether. To confirm whether the lanthanide nitrate complexes are stable in solution, we obtained the positive-ion ESI mass spectra of the Tb nitrate complex in methanol–acetonitrile solution. The ESI mass spectrum displayed a dominant peak corresponding to the $Ln_2\mathbf{L}_2$ species, namely $[Tb_2\mathbf{L}_2(NO_3)_6(CH_3OH)H]^+$ (*m*/*z* 1948.8). This observation strongly indicates that the lanthanide nitrate complexes are stable in solution. The lanthanide picrate complexes are soluble in DMF, DMSO, and acetone, slightly soluble in methanol, ethanol, acetonitrile, but insoluble in $CHCl_3$ and diethyl ether. The positive-ion ESI mass spectra of the Eu picrate complex was obtained in DMF–methanol solution. The ESI mass spectrum displayed a dominant peak corresponding to $[Eu\mathbf{L}(pic)_3(CH_3CH_2OH)(DMF)H]^+$ (*m*/*z* 1569.5), which indicates that the lanthanide picrate complexes are stable in solution. The complexes have been well characterized by FT-IR spectroscopy and elemental analyses. The IR spectrum of the free ligand displays the characteristic absorption of a carbonyl group at 1636 cm^{-1}. In comparison with the free ligand, the absence of the band at 1636 cm^{-1}, which is replaced by a new band at 1611–1614 cm^{-1} for the complexes, indicates that the oxygen atom of the carbonyl group takes part in coordination to the lanthanide ions. Accordingly, single-crystal X-ray structure analyses confirmed their structures. Unfortunately, it was not possible to grow a suitable single crystal of the Gd nitrate complex. The powder X-ray diffraction patterns for Gd and Tb (**4**) nitrate complexes are similar, thus implying that they are isostructural (Fig. S1, ESI†).

Crystal structures of 1–5

The single-crystal X-ray analyses of the complexes reveal that they are isostructural dinuclear structures with the central metal Pr, Sm, Eu, Tb, or Dy atom coordinated with nine donor atoms, six of which belong to the three bidentate nitrate groups and two oxygen atoms from carbonyl groups from two bridging ligands and the remaining one to a carbonyl group of a DMF molecule. The molecular structure of the complex **4** is shown in Fig. 1. The crystal structure analyses provide direct evidence that the complexes **1–5** form discrete [2+2] rectangular macrocycles whose sizes are 9.840 × 7.869 Å (**1**), 9.797 × 7.830 Å (**2**), 9.775 × 7.821 Å (**3**), 9.745 × 7.805 Å (**4**) and 9.729 Å × 7.783 Å (**5**), respectively.

As shown in Fig. 1a, two ligands adopt a face-to-face orientation and are joined together by two Tb(III) ions to generate a discrete zero-dimensional (0D) binuclear rectangular macrocycle structure. The unit consists of two independent enantiomeric Tb(III) centers bridged by two ligands. As shown in Fig. S2 (ESI†), two ligands are connected with each other by intramolecular π–π interactions of the two benzene ring planes of the arms which are parallel with each other with the centroid to centroid distance of 3.578 Å, and two benzene rings of two arms

Table 1 Elemental analytical and IR spectral data of the complexes in solid state

Complexes	Found (Calcd.)%			IR (C=O) (cm^{-1})
	C	H	N	
$[PrL(NO_3)_6]\cdot 2H_2O$	48.12 (47.96)	4.30 (4.44)	8.25 (8.60)	1613
$[SmL(NO_3)_3]\cdot H_2O$	48.75 (48.38)	4.44 (4.27)	8.06 (8.68)	1613
$[EuL(NO_3)_3]\cdot H_2O$	48.45 (48.30)	4.43 (4.26)	9.01 (8.62)	1614
$[GdL(NO_3)_3]\cdot H_2O$	48.40 (48.04)	4.47 (4.24)	9.00 (8.62)	1613
$[TbL(NO_3)_3]\cdot H_2O$	47.97 (47.96)	4.40 (4.23)	9.01 (8.60)	1614
$[DyL(NO_3)_3]\cdot H_2O$	47.59 (47.78)	4.34 (4.22)	8.09 (8.57)	1614
$[NdL(pic)_3]\cdot H_2O$	46.92 (46.88)	3.33 (3.24)	11.17 (11.51)	1612
$[EuL(pic)_3]\cdot 2H_2O$	46.21 (46.07)	3.08 (3.32)	11.40 (11.31)	1611
$[TbL(pic)_3]\cdot H_2O$	46.50 (46.42)	3.27 (3.21)	11.08 (11.40)	1611
$[ErL(pic)_3]\cdot H_2O$	46.20 (46.16)	3.08 (3.19)	10.98 (11.33)	1612

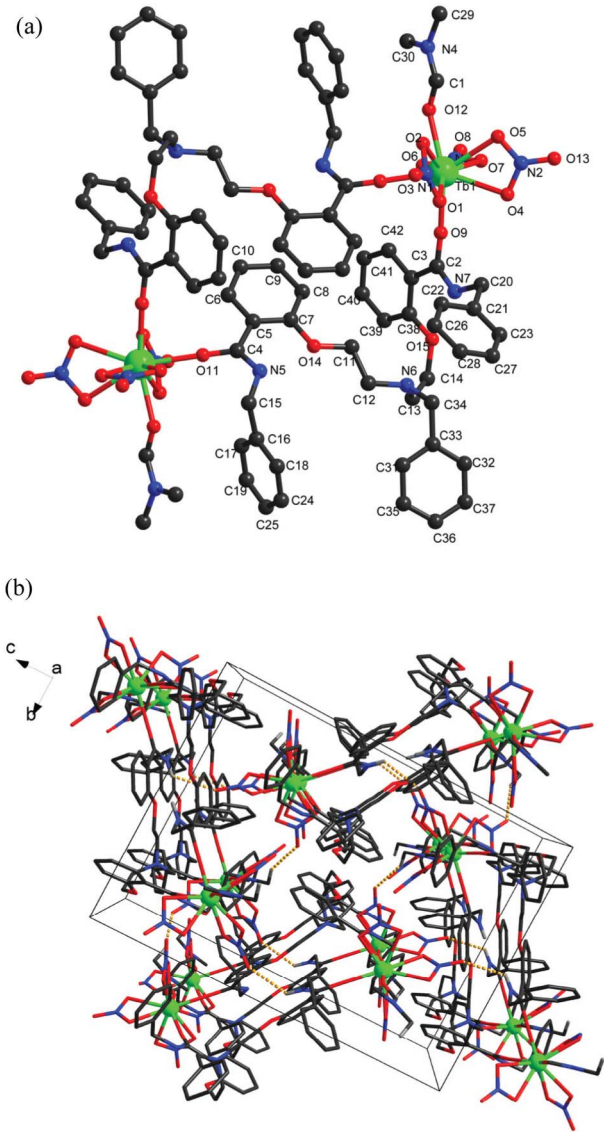

Fig. 1 (a) The molecular structure and atom labeling schemes of compound **4**. (b) An illustration of intermolecular hydrogen bonds (yellow dashed lines) in the 3D supramolecular architectures in **4**. (The hydrogen atoms without formed hydrogen bonds and the benzyl groups of the ligands are omitted for clarity.)

of each ligand interact with each other through C–H···π interactions referred as a T-shape arrangement. The Tb(III) ions have a TbO_9 coordination environment, forming a distorted tricapped trigonal prism. The distance of Tb–Tb is 13.016 Å. In addition, the dinuclear complex was assembled into a three-dimensional (3D) net-like supramolecular structure by intermolecular hydrogen bonds (Fig. 1b). Hydrogen bonding parameters of complex **4** are given in Table S4 (ESI†).

Crystal structures of 6–9

To explore the role of different anions in the self-assembly process, picrate, with a larger size, was used instead of nitrate to carry out the reaction. The single-crystal X-ray analyses reveal that the coordination environments of Nd(III) and Eu(III) are nine-coordinated in compounds **6**, **7** and those of Tb(III) and Er(III) are eight-coordinated in compounds **8**, **9**. They all possess the same one-dimensional (1D) linear coordination polymeric structures. As shown in Fig. 2, the Eu(III) ion in complex **7** has a nine-coordinate environment, six of which are occupied by six oxygen atoms from three bidentate picrate groups, two belong to the oxygen atoms of carbonyl groups of two ligands and the remaining one to coordinated ethanol molecule, forming a distorted tricapped trigonal prism. The Tb(III) and Er(III) ions in compounds **8** and **9** possess very similar coordination environments compared with those of Nd(III) and Eu(III), except that one bidentate picrate group that occurs in **6** or **7** was replaced by one monodentate picrate group in **8** or **9** (Fig. 3a). Eight-coordinate complexes are known in a variety of coordination geometries for which the assignment to the closest idealized polyhedron usually is not straightforward. For the eight-coordinate geometry, the three most common idealized coordination polyhedra correspond to the

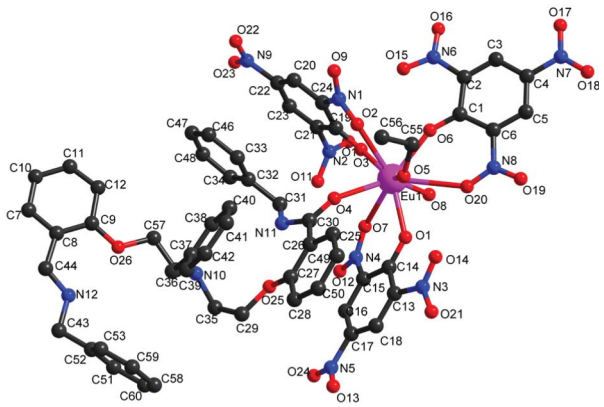

Fig. 2 The local coordination environment of Eu(III) in compound **7**. (The hydrogen atoms are omitted for clarity.)

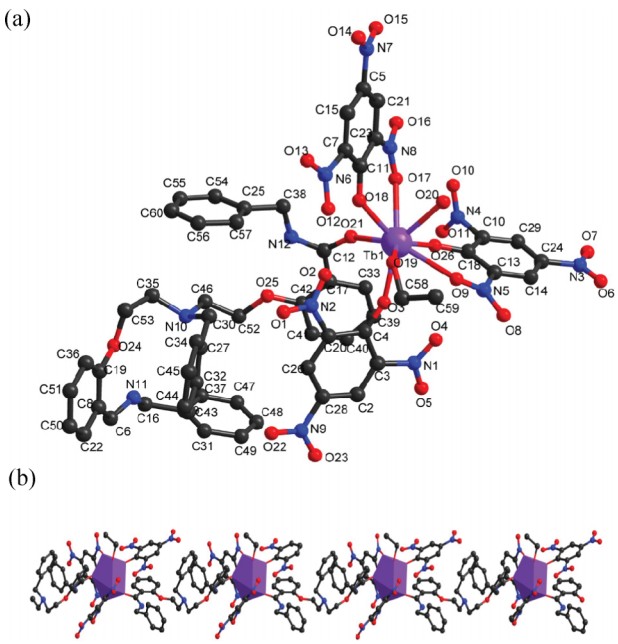

Fig. 3 (a) The local coordination environment of Tb(III) in compound **8**. (b) A 1D linear coordination polymer chain of compound **8**.

bicapped trigonal prism (C_{2v}), square antiprism (D_{4d}), and trigonal dodecahedron (D_{2d}). In order to estimate the degree of the distorted coordination structures of Tb(III) and Er(III) complexes, we carried out calculations based on the "shape-measure" criterion S.[10] The lowest value of S for the three pairs represents the best fit to the closest idealized geometry, and the resulting shape measure calculations for the two complexes studied herein are summarized in Table S5 (ESI†). It is readily apparent that the most common matches for the two complexes were both the distorted bicapped trigonal prism (C_{2v}). Therefore, only [Tb**L**(pic)$_3$(CH$_3$CH$_2$OH)]$_n$ is selected for investigation here in detail as a representative example. The Tb–O distances are between 2.232(4) and 2.584(5) Å, which are comparable to the corresponding Tb–O bond lengths found in related complexes.[3b,11] Each ligand binds to two Tb(III) ions using its two oxygen atoms of the amide groups. So the whole structure consists of an infinite array of Tb(III) ions bridged by bidentate ligands and a one-dimensional (1D) linear coordination polymer formed (Fig. 3b). The weak intermolecular hydrogen bonds C(40)–H(40)···O(15) and C(60)–H(60)···O(4) in complex **8** link the 1D chains into a two-dimensional (2D) layer supramolecular structure, as shown in Fig. S3a (ESI†). In addition, the layers are linked by weak intermolecular hydrogen bonds C(35)–H(35A)···O(10), C(37)–H(37)···O(16), C(51)–H(51)···O(1) and C(58)–H(58B)···O(23) to form an infinite three-dimensional (3D) supramolecular structure (Fig. S3b, ESI†). The single-crystal X-ray analysis reveals that a coordinated ethanol molecule exists in the lanthanide picrate complex, which may quench lanthanide luminescence.

Anion influence on structures of lanthanide coordination compounds

For further careful investigation of the self-assembly between Ln(NO$_3$)$_3$·6H$_2$O, Ln(pic)$_3$·6H$_2$O and the ligands, nine lanthanide coordination compounds were isolated. Herein, [Tb$_2$**L**$_2$(NO$_3$)$_6$(DMF)$_2$]$_n$ (**4**) and [Tb**L**(pic)$_3$(CH$_3$CH$_2$OH)]$_n$ (**8**) are representatively discussed in detail. Calculation using PLATON[13] reveals that the nitrates and picrates account for about 12.7 and 41.7% of the crystal volumes in compounds **4** and **8**, respectively. A deeper view of compound **4** indicates that the angle of O(9)–Tb(1)–O(11) is 80.5°, which is relatively easy to form into the 2 : 2 mode dinuclear metallomacrocycle through the connectivity of two ligand bridges; however, in compound **8**, the angle of O(20)–Tb(1)–O(21) is 135.4°, which could not easily form a 2 : 2 mode complex owing to the larger steric confinement of the picrates. (O(9), O(11), O(20) and O(21) are coordinated oxygen atoms of carbonyl groups of the ligands.) Therefore, it forms a one-dimensional (1D) chain pattern through opening one ring. A better insight into the nature of the involved structures can be achieved from Scheme 2. Under the same conditions of the solution, a DMF molecule was coordinated to **4** but an ethanol one to **8**. The volumes of DMF and ethanol molecules calculated by PLATON[12] are 10.7 and 2.2%, respectively. We speculated that the variations of coordinated solvent molecules from the DMF in **4** to ethanol in **8** are also attributed to the different steric confinement of nitrates and picrates. So we unequivocally presume that the size of the anions plays a prominent role in the architecture of lanthanide coordination compounds. Besides this, with the increasing atomic number of the lanthanide, the coordination

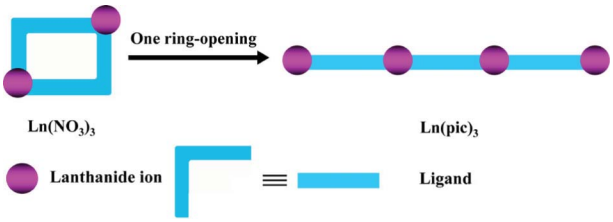

Scheme 2 A schematic view of the variations from zero- to one-dimensional structures.

numbers of lanthanide ions were reduced from nine in **6** and **7** to eight in **8** and **9** under the same conditions, which is attributed to lanthanide contraction effects.

Luminescent properties of the compounds 2–5

Lanthanide complexes are known for their photoluminescent properties. The luminescence of lanthanide complexes is produced through three steps. First, exciting-light energy is absorbed by the organic ligands attached to Ln(III), energy is then transferred into one or several excited states of the central Ln(III) ions, and, finally, the Ln(III) emits characteristic and narrow light. In the second step, efficient energy transfer from ligand to Ln(III) is one of key factors to achieve characteristic lanthanide luminescence.[13] We have studied the luminescent properties of the nitrate and picrate complexes, and we found that the picrate complexes give very weak luminescence. We presume that this phenomenon might be due to coordinated ethanol molecules existing in lanthanide picrate complexes, which decrease the luminescence intensity and overall luminescence quantum yields, as the thermal oscillator of the hydroxyl group of ethanol molecules will consume some excitation energy absorbed by "antenna" ligands.[14] So, we herein only discuss the luminescent properties of compounds **2–5** in detail.

Excited by the absorption band at 323 nm, the "free" ligand exhibits broad emission bands (λ_{max} = 438 nm) in the solid state. The excitation and luminescence emission spectra of the zero-dimensional dinuclear complexes **2–5** in the solid state (Fig. 4a–d) were recorded at room temperature, and the relevant photophysical data are summarized in Table 2. For **2**, the combined excitation and emission spectra are presented in Fig. 4a. The excitation spectrum was obtained by monitoring the 596 nm line of the $^4G_{5/2}\rightarrow{}^6H_{7/2}$ emission. The emission intensity is the weakest, but two characteristic bands can still be observed, which are attributed to $^4G_{5/2}\rightarrow{}^6H_J$ (J = 5/2, 7/2) transitions. Compound **3** exhibits red luminescence, which arises from the $^5D_0\rightarrow{}^7F_2$ transition of Eu(III) ion, as shown in Fig. 4b. The excitation spectrum of complex **3** shows that the excitation energy is mainly absorbed by the $^5D_4$, $^5G_{0\text{-}4}$, $^5L_6$, $^5D_{2,1}$ levels of the central Eu(III) ion (see Fig. 4b).[15] The weak ligand-localized ($S_0\rightarrow S_1$) excitation band proves that luminescence sensitization *via* direct excitation of the ligands is not promising. There are five characteristic peaks of Eu(III) shown in the emission spectrum which are attributed to $^5D_0\rightarrow{}^7F_0$ (579 nm), $^5D_0\rightarrow{}^7F_1$ (592 nm), $^5D_0\rightarrow{}^7F_2$ (614 nm), $^5D_0\rightarrow{}^7F_3$ (651 nm), $^5D_0\rightarrow{}^7F_4$ (691 nm). The intensity of the $^5D_0\rightarrow{}^7F_2$ transition (electric dipole) is stronger than that of the $^5D_0\rightarrow{}^7F_1$ transition (magnetic dipole), and it indicates that the coordination environment of the

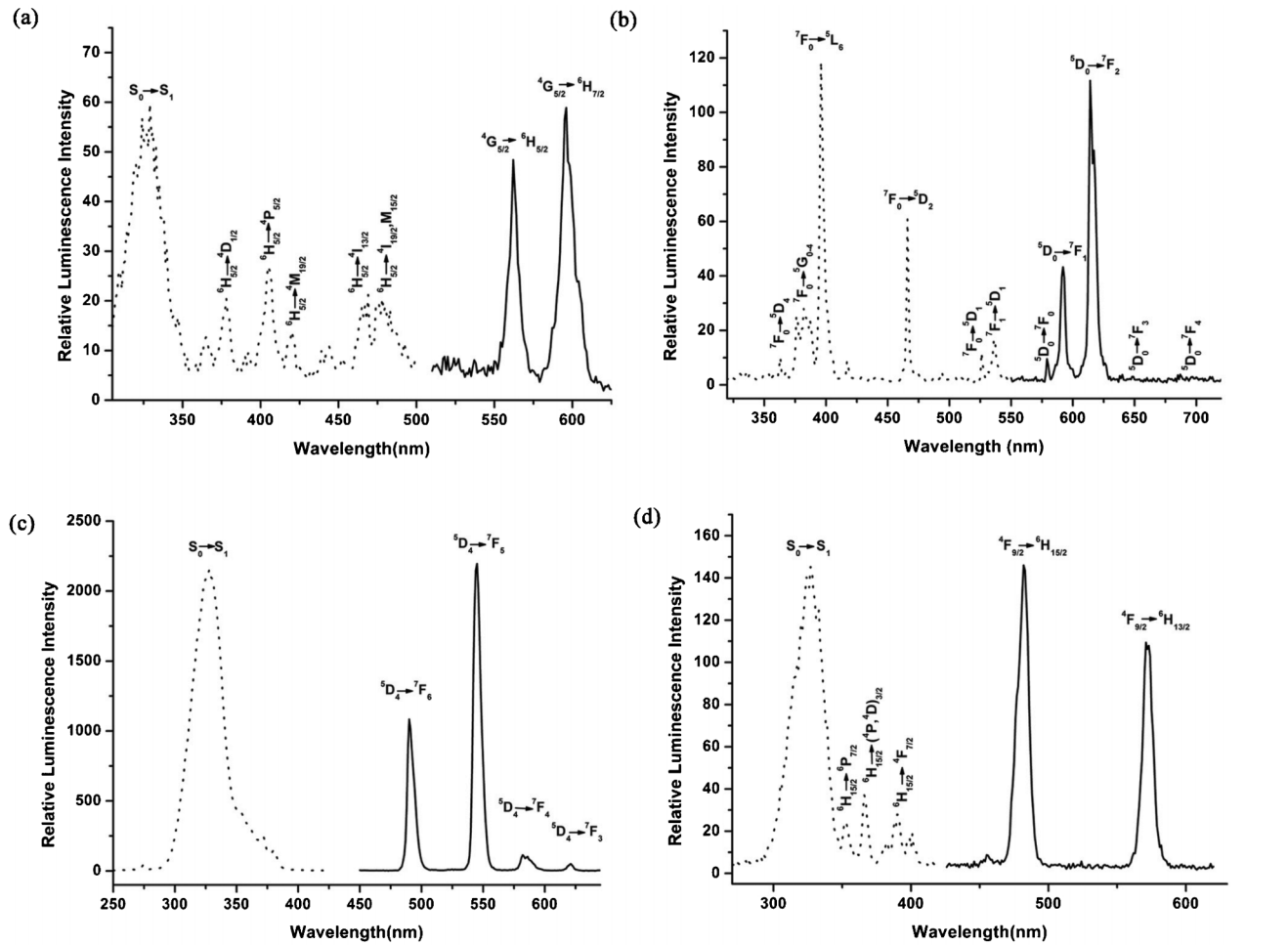

Fig. 4 Room-temperature excitation and emission spectra of (a) **2** (λ_{ex} = 329 nm), (b) **3** (λ_{ex} = 396 nm), (c) **4** (λ_{ex} = 327 nm), and (d) **5** (λ_{ex} = 327 nm) in the solid state.

Table 2 Photophysical characterization of compounds **2–5**

Compounds	λ_{ex} (nm)	λ_{em} (nm)	Assignment	τ (ms)	$\Phi_{overall}$ (%)
2	329	562	$^4G_{5/2}\rightarrow{}^6H_{5/2}$	0.047 ± 0.001	1.1
		596	$^4G_{5/2}\rightarrow{}^6H_{7/2}$		
3	396	579	$^5D_0\rightarrow{}^7F_0$	1.072 ± 0.001	2.4
		592	$^5D_0\rightarrow{}^7F_1$		
		614	$^5D_0\rightarrow{}^7F_2$		
		651	$^5D_0\rightarrow{}^7F_3$		
		691	$^5D_0\rightarrow{}^7F_4$		
4	327	490	$^5D_4\rightarrow{}^7F_6$	1.346 ± 0.001	50
		545	$^5D_4\rightarrow{}^7F_5$		
		582	$^5D_4\rightarrow{}^7F_4$		
		620	$^5D_4\rightarrow{}^7F_3$		
5	327	483	$^4F_{9/2}\rightarrow{}^6H_{15/2}$	0.050 ± 0.001	7.0
		572	$^4F_{9/2}\rightarrow{}^6H_{13/2}$		

Eu(III) ion is devoid of an inversion center,[16] which is consistent with the crystallographic analyses. For **4**, the excitation spectrum exhibits a broad excitation band (BEB) between 280 and 400 nm, which is associated with the electronic transitions of the ligand (Fig. 4c). This proves that the luminescence sensitization *via* excitation of the ligand is effective in the case of the Tb(III) complex. The emission intensity of **4** is stronger than that of the other three under the same conditions. There are four characteristic peaks shown in Fig. 4c, which result from the $^5D_4\rightarrow{}^7F_J$ (J = 6, 5, 4, 3) transitions. For **5**, there are two characteristic bands that can be seen in the emission spectrum, which are attributed to transitions of 483 nm ($^4F_{9/2}\rightarrow{}^6H_{15/2}$), and 572 nm ($^4F_{9/2}\rightarrow{}^6H_{13/2}$) (Fig. 4d).

The overall luminescence quantum yields, $\Phi_{overall}$, of **2–5** in the solid state were found to be 1.1, 2.4, 50, and 7.0% using an integrating sphere when excited at 329, 327, 327, and 327 nm, respectively. The luminescence lifetime values of **2–5** were determined to be 0.047 ± 0.001, 1.072 ± 0.001, 1.346 ± 0.001, and 0.050 ± 0.001 ms from the luminescent decay profiles at room temperature by fitting with a monoexponential curve (Figs S4–S7, ESI†), indicating the presence of single chemical environment around the emitting Ln(III) ion.

Comparing the relative intensity and overall luminescence quantum yield of four complexes, we could find that they follow the trend **4** > **5** > **3** > **2**, which means that the energy transfer from the ligands to Eu(III) and Sm(III) is less effective than that to Tb(III) and Dy(III). This behaviour can be explicated by the ligand-to-metal energy migration pathways discussed below. In addition, the luminescence excitation and emission spectra of the

Tb(III) nitrate complex in methanol, ethanol, acetone, DMF and DMSO solutions were recorded at room temperature (Fig. S8, ESI†). The characteristic emission bands of Tb(III) can be observed in the emission spectra, which indicated that the lanthanide nitrate complexes survive in solution.

Energy transfer between the ligand and Ln(III)

To elucidate the energy migration pathways in these lanthanide complexes, it was necessary to determine the singlet and triplet energy levels of the ligand, which were estimated by referring to their wavelengths of UV-vis absorbance edges and the lower wavelength emission edges of the corresponding phosphorescence spectra. The wavelength of absorbance edge of the ligand **L** is 318 nm (Fig. S9, ESI†), indicating that the singlet energy level (S_1) of the ligand is 31 446 cm^{-1}. A triplet excited state T_1, which is localized on one ligand only and is independent of the lanthanide nature.[17] In order to acquire the triplet excited state T_1 of the ligand, the phosphorescence spectrum of the compound $[GdL(NO_3)_6]\cdot H_2O$ was measured at 77 K in a methanol–ethanol mixture (v : v = 1 : 1) (Fig. S10, ESI†),[18] and the triplet state energy level T_1 of the ligand is 24 331 cm^{-1}. It is interesting to note that the triplet state energy level T_1 of the newly designed ligand lies well above the lowest excited resonance level $^4G_{5/2}$ of Sm(III) (17 900 cm^{-1}), $^5D_0$ of Eu(III) (17 300 cm^{-1}), $^5D_4$ of Tb(III) (20 500 cm^{-1}) and $^4F_{9/2}$ of Dy(III) (21 000 cm^{-1}), therefore indicating that the ligand can act as an antenna for the photosensitization of Sm(III), Eu(III), Tb(III) or Dy(III) ions. According to Reinhoudt's empirical rule,[19] an efficient ligand-to-metal energy transfer requires good S_1–T_1 intersystem crossing, which becomes effective when the energy difference between these states is at least 5000 cm^{-1}, and the energy gap between S_1 and T_1 for the ligand **L** amounts to 7115 cm^{-1}. Thus, this newly designed ligand has relatively good intersystem crossing efficiency. On the other hand, an intramolecular energy transfer from the triplet state level of the ligand to the resonance level of the Ln(III) ion is one of the most important processes having influence on the Ln(III) luminescence. It is therefore necessary that there exists a suitable energy gap between the ligand-centered triplet state and the lanthanide ion emissive states. Latva's empirical rule[17,20] states that an optimal ligand-to-metal energy transfer process for Eu(III) needs $\Delta E = E(T_1) - E(^5D_0)$ = 2500–4000 cm^{-1} and for Tb(III) $\Delta E = E(T_1) - E(^5D_4)$ = 2500–4500 cm^{-1}. The energy gaps between ligand and lanthanide-centered levels are 3831 cm^{-1} ($\Delta E = T_1$–$^5D_4$) for Tb(III) and 3331 cm^{-1} ($\Delta E = T_1$–$^4F_{9/2}$) for Dy(III), which facilitates efficient energy transfer.[17b] By contrast, the energy gaps between ligand and lanthanide-centered levels are 7031 cm^{-1} for Eu(III) and 6431 cm^{-1} for Sm(III), respectively. Following the method described in the literature,[21] it is possible to evaluate that the sensitization efficiency of the ligand (η_{sens}) for Eu(III) complex is 10.4% on the basis of the luminescence data (emission spectrum and $^5D_0$ lifetime) (Table S6, ESI†). The poor sensitization efficiency of the ligand (η_{sens}) indicated luminescence sensitization of the Eu(III) complex *vis* excitation of the ligand is not efficient, which is mainly because of the larger energy gap between the triplet state and $^5D_0$ level of Eu(III). This therefore supports the observation of stronger sensitization of **4** and **5** than **2** and **3**.

Conclusions

As a continuing project in our laboratory about the development of lanthanide complexes generated from various amide type ligands and lanthanide salts, we successfully designed and synthesized ten new lanthanide supramolecular architectures based on a new amide type ligand **L** (**L** = benzyl-*N*,*N*-bis[(2′-benzylaminofomyl)phenoxyl)ethyl]-amine) in this report. The single-crystal X-ray diffraction analyses reveal that the complexes $[Ln_2L_2(NO_3)_6(DMF)_2]_n$ are isostructural zero-dimensional (0D) dinuclear rectangular macrocycle structures, while the compounds $[LnL(pic)_3(CH_3CH_2OH)]_n$ exhibit one-dimensional (1D) chain coordination polymers. The variations from zero- to one-dimensional coordination structures are attributed to different steric confinement of the nitrate and picrate anions. We have also studied the solid state luminescent properties of the nitrate and picrate complexes, and found that the picrate complexes give very weak luminescence due to coordinated ethanol molecules decreasing the luminescence. so we only investigated the luminescent properties of the lanthanide nitrate complexes in this report. Under the excitation, the four complexes **2–5** can all show the characteristic luminescent emissions of Sm(III), Eu(III), Tb(III) or Dy(III). The relative intensity and overall luminescence quantum yield changes in the order of **4** > **5** > **3** > **2**, which shows the ligands can effectively sensitize the luminescence of Tb(III) and Dy(III) rather than Eu(III) and Sm(III). In addition, the ligand-to-metal energy migration pathways studies also make it rational. This work is hoped to afford inspiration for the construction of lanthanide-based photonic devices.

Acknowledgements

This work was financially supported by the National Natural Science Foundation of China (Project 20931003, 21071068) and the Fundamental Research Funds for the Central Universities (Project lzujbky-2012-k08).

References

1 (*a*) J. T. Hupp and K. R. Poeppelmeier, *Science*, 2005, **309**, 2008; (*b*) N. L. Rosi, J. Eckert, M. Eddaoudi, D. T. Vodak, J. Kim, M. O'Keeffe and O. M. Yaghi, *Science*, 2003, **300**, 1127; (*c*) J. S. Seo, D. Whang, H. Lee, S. I. Jun, J. Oh, Y. J. Jeon and K. Kim, *Nature*, 2000, **404**, 982; (*d*) N. Nijem, J.-F. Veyan, L. Kong, K. Li, S. Pramanik, Y. Zhao, J. Li, D. Langreth and Y. J. Chabal, *J. Am. Chem. Soc.*, 2010, **132**, 1654; (*e*) H.-L. Jiang, Y. Tatsu, Z.-H. Lu and Q. Xu, *J. Am. Chem. Soc.*, 2010, **132**, 5586; (*f*) D. Zhao, D.-Q. Yuan, D.-F. Sun and H.-C. Zhou, *J. Am. Chem. Soc.*, 2009, **131**, 9186; (*g*) A. o. Yazaydın, R. Q. Snurr, T.-H. Park, K. Koh, J. Liu, M. D. LeVan, A. I. Benin, P. Jakubczak, M. Lanuza, D. B. Galloway, J. J. Low and R. R. Willis, *J. Am. Chem. Soc.*, 2009, **131**, 18198; (*h*) L. Pan, M. B. Sander, X. Huang, J. Li, M. Smith, E. Bittner, B. Bockrath and J. K. Johnson, *J. Am. Chem. Soc.*, 2004, **126**, 1308; (*i*) L. Pan, H. Liu, X. Lei, X. Huang, D. H. Olson, N. J. Turro and J. Li, *Angew. Chem., Int. Ed.*, 2003, **42**, 542; (*j*) G. Férey, M. Latroche, C. Serre, F. Millange, T. Loiseau and A. Percheron-Guégan, *Chem. Commun.*, 2003, 2976; (*k*) D. N. Dybtsev, H. Chun, S. H. Yoon, D. Kim and K. Kim, *J. Am. Chem. Soc.*, 2003, **126**, 32; (*l*) K. S. Min and M. P. Suh, *Chem.–Eur. J.*, 2001, **7**, 303; (*m*) A. Rodriguez-Dieguez, A. Salinas-Castillo, A. Sironi, J. M. Seco and E. Colacio, *CrystEngComm*, 2010, **12**, 1876; (*n*) K. S. Min and M. P. Suh, *J. Am. Chem. Soc.*, 2000, **122**, 6834; (*o*) L. G. Beauvais, M. P. Shores and J. R. Long, *J. Am. Chem. Soc.*, 2000, **122**, 2763; (*p*) K.-L. Hou, F.-Y. Bai, Y.-H. Xing, J.-L. Wang and Z. Shi, *CrystEngComm*, 2011, **13**, 3884.

2 (*a*) Z.-H. Zhang, Y. Song, T.-a. Okamura, Y. Hasegawa, W.-Y. Sun and N. Ueyama, *Inorg. Chem.*, 2006, **45**, 2896; (*b*) A. Nag, P. J. Schmidt and W. Schnick, *Chem. Mater.*, 2006, **18**, 5738; (*c*) C. M. Rudzinski, A. M. Young and D. G. Nocera, *J. Am. Chem. Soc.*, 2002, **124**, 1723; (*d*) H. Nozary, C. Piguet, J.-P. Rivera, P. Tissot, P.-Y. Morgantini, J. Weber, G. Bernardinelli, J.-C. G. Bünzli, R. Deschenaux, B. Donnio and D. Guillon, *Chem. Mater.*, 2002, **14**, 1075; (*e*) K. Binnemans and C. Görller-Walrand, *Chem. Rev.*, 2002, **102**, 2303; (*f*) B. Cai, P. Yang, J.-W. Dai and J.-Z. Wu, *CrystEngComm*, 2011, **13**, 985.

3 (*a*) X.-H. Yan, Z.-H. Cai, C.-L. Yi, W.-S. Liu, M.-Y. Tan and Y. Tang, *Inorg. Chem.*, 2011, **50**, 2346; (*b*) Y.-L. Guo, W. Dou, X.-Y. Zhou, W.-S. Liu, W.-W. Qin, Z.-P. Zang, H.-R. Zhang and D.-Q. Wang, *Inorg. Chem.*, 2009, **48**, 3581; (*c*) D.-Y. Liu, Z.-Q. Kou, Y.-F. Li, K.-Z. Tang, Y. Tang, W.-S. Liu and M.-Y. Tan, *Inorg. Chem. Commun.*, 2009, **12**, 461; (*d*) S. Petoud, S. M. Cohen, J.-C. G. Bünzli and K. N. Raymond, *J. Am. Chem. Soc.*, 2003, **125**, 13324; (*e*) X.-Q. Song, X.-Y. Zhou, W.-S. Liu, W. Dou, J.-X. Ma, X.-L. Tang and J.-R. Zheng, *Inorg. Chem.*, 2008, **47**, 11501; (*f*) Q. Wang, K.-Z. Tang, W.-S. Liu, Y. Tang and M.-Y. Tan, *Eur. J. Inorg. Chem.*, 2010, **2010**, 5318; (*g*) G. Zucchi, A.-C. Ferrand, R. Scopelliti and J.-C. G. Bünzli, *Inorg. Chem.*, 2002, **41**, 2459; (*h*) X.-H. Yan, Y.-F. Li, Q. Wang, X.-G. Huang, Y. Zhang, C.-J. Gao, W.-S. Liu, Y. Tang, H.-R. Zhang and Y.-L. Shao, *Cryst. Growth Des.*, 2011, **11**, 4205; (*i*) A. G. Blackman, *Polyhedron*, 2005, **24**, 1; (*j*) L. S. Reddy, S. Basavoju, V. R. Vangala and A. Nangia, *Cryst. Growth Des.*, 2005, **6**, 161.

4 (*a*) Y. Wang, X.-Q. Zhao, W. Shi, P. Cheng, D.-Z. Liao and S.-P. Yan, *Cryst. Growth Des.*, 2009, **9**, 2137; (*b*) J.-P. Costes, B. Donnadieu, R. Gheorghe, G. Novitchi, J.-P. Tuchagues and L. Vendier, *Eur. J. Inorg. Chem.*, 2008, **2008**, 5235; (*c*) J. Xie, Y.-Q. Huang, T.-a. Okamura, W.-Y. Sun and N. Ueyama, *Z. Anorg. Allg. Chem.*, 2007, **633**, 1211; (*d*) X.-F. Wang, Y. Lv, Z. Su, T.-a. Okamura, G. Wu, W.-Y. Sun and N. Ueyama, *Z. Anorg. Allg. Chem.*, 2007, **633**, 2695; (*e*) D.-L. Long, R. J. Hill, A. J. Blake, N. R. Champness, P. Hubberstey, C. Wilson and M. Schröder, *Chem.–Eur. J.*, 2005, **11**, 1384; (*f*) Y.-B. Dong, J.-Y. Cheng, R.-Q. Huang, M. D. Smith and H.-C. zur Loye, *Inorg. Chem.*, 2003, **42**, 5699; (*g*) A. Jouaiti, V. Jullien, M. W. Hosseini, J.-M. Planeix and A. De Cian, *Chem. Commun.*, 2001, 1114; (*h*) N. R. Brooks, A. J. Blake, N. R. Champness, J. W. Cunningham, P. Hubberstey, S. J. Teat, C. Wilson and M. Schröder, *J. Chem. Soc., Dalton Trans.*, 2001, 2530; (*i*) M.-L. Tong, S.-L. Zheng and X.-M. Chen, *Chem.–Eur. J.*, 2000, **6**, 3729 (*j*) M. A. Withersby, A. J. Blake, N. R. Champness, P. Hubberstey, W.-S. Li and M. Schröder, *Angew. Chem., Int. Ed. Engl.*, 1997, **36**, 2327; (*k*) F.-J. Liu, D. Sun, H.-J. Hao, R.-B. Huang and L.-S. Zheng, *Cryst. Growth Des.*, 2012, **12**, 354; (*l*) M. Du, X.-H. Bu, Y.-M. Guo, H. Liu, S. R. Batten, J. Ribas and T. C. W. Mak, *Inorg. Chem.*, 2002, **41**, 4904; (*m*) M. Du, Y.-M. Guo, S.-T. Chen, X.-H. Bu, S. R. Batten, J. Ribas and S. Kitagawa, *Inorg. Chem.*, 2004, **43**, 1287.

5 M. Kondo, *Bull. Chem. Soc. Jpn.*, 1976, **49**, 2679.

6 (*a*) N. L. S. Yue, M. C. Jennings and R. J. Puddephatt, *Inorg. Chem.*, 2005, **44**, 1125; (*b*) L. Dobrzańska, G. O. Lloyd, H. G. Raubenheimer and L. J. Barbour, *J. Am. Chem. Soc.*, 2005, **128**, 698; (*c*) C. J. Kuehl, S. D. Huang and P. J. Stang, *J. Am. Chem. Soc.*, 2001, **123**, 9634.

7 N. Kazuharu, A. Kayoko, M. Hifumi, I. Yoshihisa and H. Tadao, *Bull. Chem. Soc. Jpn.*, 1987, **60**, 2037.

8 Y.-C. Tian, Y.-Q. Liang and J.-Z. Ni, *Chin. Univ. Chem. J.*, 1988, **9**, 113.

9 (*a*) G. M. Sheldrick, *Acta Crystallogr., Sect. A: Found. Crystallogr.*, 1990, **46**, 467; (*b*) G. M. Sheldrick, *SHELXS-97, A Program for X-ray Crystal Structure Solution, and SHELXL-97, A Program for X-ray Structure Refinement*, Göttingen University, Germany, 1997.

10 J. Xu, E. Radkov, M. Ziegler and K. N. Raymond, *Inorg. Chem.*, 2000, **39**, 4156.

11 W. Huang, D. Wu, P. Zhou, W. Yan, D. Guo, C. Duan and Q. Meng, *Cryst. Growth Des.*, 2009, **9**, 1361.

12 A. L. Spek, *PLATON*, Utrecht University: Utrecht, The Netherlands, 2003.

13 (*a*) F. Aiga, H. Iwanaga and A. Amano, *J. Phys. Chem. A*, 2005, **109**, 11312; (*b*) P. He, H.-H. Wang, S.-G. Liu, J.-X. Shi, G. Wang and M.-L. Gong, *Inorg. Chem.*, 2009, **48**, 11382; (*c*) M. D. Regulacio, M. H. Pablico, J. A. Vasquez, P. N. Myers, S. Gentry, M. Prushan, S.-W. Tam-Chang and S. L. Stoll, *Inorg. Chem.*, 2008, **47**, 1512; (*d*) C. Bazzicalupi, A. Bencini, A. Bianchi, C. Giorgi, V. Fusi, A. Masotti, B. Valtancoli, A. Roque and F. Pina, *Chem. Commun.*, 2000, 561; (*e*) N. Sabbatini, M. Guardigli and J.-M. Lehn, *Coord. Chem. Rev.*, 1993, **123**, 201.

14 (*a*) A. R. Ramya, M. L. P. Reddy, A. H. Cowley and K. V. Vasudevan, *Inorg. Chem.*, 2010, **49**, 2407; (*b*) S. Sivakumar, M. L. P. Reddy, A. H. Cowley and K. V. Vasudevan, *Dalton Trans.*, 2010, **39**, 776.

15 M. Albin, R. R. Whittle and W. D. Horrocks, *Inorg. Chem.*, 1985, **24**, 4591.

16 A. F. Kirby, D. Foster and F. S. Richardson, *Chem. Phys. Lett.*, 1983, **95**, 507.

17 (*a*) M. Latva, H. Takalo, V.-M. Mukkala, C. Matachescu, J. C. Rodríuez-Ubis and J. Kankare, *J. Lumin.*, 1997, **75**, 149; (*b*) F. Gutierrez, C. Tedeschi, L. Maron, J.-P. Daudey, R. Poteau, J. Azema, P. Tisnès and C. Picard, *Dalton Trans.*, 2004, 1334.

18 W. R. Dawson, J. L. Kropp and M. W. Windsor, *J. Chem. Phys.*, 1966, **45**, 2410.

19 F. J. Steemers, W. Verboom, D. N. Reinhoudt, E. B. van der Tol and J. W. Verhoeven, *J. Am. Chem. Soc.*, 1995, **117**, 9408.

20 N. Arnaud and J. Georges, *Spectrochim. Acta, Part A*, 2003, **59**, 1829.

21 (*a*) S. V. Eliseeva and J.-C. G. Bunzli, *Chem. Soc. Rev.*, 2010, **39**, 189; (*b*) N. M. Shavaleev, S. V. Eliseeva, R. Scopelliti and J.-C. G. Bünzli, *Inorg. Chem.*, 2010, **49**, 3927; (*c*) M. H. V. Werts, R. T. F. Jukes and J. W. Verhoeven, *Phys. Chem. Chem. Phys.*, 2002, **4**, 1542; (*d*) M. Fernandes, V. de Zea Bermudez, R. A. Sá Ferreira, L. D. Carlos, A. Charas, J. Morgado, M. M. Silva and M. J. Smith, *Chem. Mater.*, 2007, **19**, 3892.

